SIMULATION STUDY ON VORTEX-INDUCED VIBRATION AIR WAKE ENERGY FOR AIRPORT RUNAWAY APPLICATION: A PRELIMINARY ANALYSIS

A.Q. Abdullah[1], A. A. Azeez[1], S.S. Dol[1*], M. S. Khan[1] and M.A.M. Said[2]

[1]Department of Mechanical Engineering, Abu Dhabi University, United Arab Emirates

[2]Department of Mechanical Engineering, Universiti Teknologi PETRONAS, Malaysia

Email: sharulshambin.dol@adu.ac.ae

ABSTRACT

The objective of this research paper is to conduct a preliminary analysis of the effects of various cylindrical cross-sectional shapes on vortex-induced vibration for airport runaway air wake energy generation. In the case of the airport runway, vortices are generated from the aeroplane bodies that exit and enter the runway during take-off and landing operations. These oscillations can be utilized to generate power due to the large fluctuations produced by the vortices. Vortex-induced vibration works on the principle of Kármán vortices where a cylindrical or bluff-body shaped object oscillates due to the alternate vortex formation on the boundary layers by adverse fluid pressure. The oscillation depends on the unsteady lift force generated. This mechanical oscillation is later converted to electrical energy. Five cylindrical cross-section cases are investigated by computational fluid dynamics (CFD) k-ω turbulence model to identify the best case that will provide the largest lift force; hence the maximum power output generation. These cases are simulated using typical take-off air speeds for jetliners in order to finalize the overall performance. The observed results show that the elliptical cross-section with 3" height and 2" length provides the best cross-section in producing the greatest amount of energy. The total power generated from a single-cylinder was 707.1 Watts. The system can be optimized for larger aeroplanes and operation frequencies as well as could be expanded for larger energy output.

Keywords: *airport runaway, lift force, oscillation, renewable, turbulence, vortex-induced vibration*

INTRODUCTION

The global demand for renewable energy is growing rapidly, especially in the transportation sector. In contrast, solar and wind energy are the mainstream renewable resources, their applications are limited and geographically constrained [1]. Vortex-induced vibration (VIV) is one of the useful alternative techniques that produce infinite oscillations from infinite flowing streams. The system consists of a spring and damper that convert or harness mechanical energy from the turbulent flow to useful energy. Vortex-induced vibration is a mechanism that interacts with a flowing fluid to produce motion or energy; most of the commonly used VIV systems utilize a cylinder with a circular cross-section. The cylinder oscillates in a specific manner when submerged in flowing fluid. The oscillations produced also depends on the fluid properties. Vortices are generated due to the viscosity generated by the friction between the fluid and the body along with the boundary layer. The pressure distribution will be varying along the body surface where different lift forces develop on each side and make the body oscillates. The Reynolds number of the free stream affects the oscillations by varying the produced forces from VIV, flow separation, and vortices [2].

Airports runways are utilized to handle a large volume of air traffics. Airport runways are full of turbulence produced from landing and take-off operations. These processes are repeated with specific frequency variations based on the size of the airport, the number of trips and the size of the aeroplanes with the specific take-off and landing speeds. Largely populated cities tend to have bigger airports and having more flights using the runways with larger aircraft. While aeroplanes arrive and depart, swirling turbulent flow will be produced. These oscillations, it could be harnessed properly, would be able to turn into useful energy for basic utility applications (e.g., lights, pumps refuelling operations, heating and ventilations at airport buildings). Flow separation (wake region) produced from aeroplanes vary based on three parameters; load, wingspan and landing and take-off speed. For example, statistically, Mumbai International airport in India (Chhatrapati Shivaji Maharaj International Airport) has one of the largest numbers of aircraft that arrive and depart the airport, with 935 trips per day and the estimated time between two aeroplanes is about 65 seconds. Therefore, even with the small amount of energy could be harnessed per VIV system, the scale can be expanded based on the large airport operations such as the Mumbai International airport can be carried out [3]. The size of upper-medium regional aeroplanes (e.g., Airbus A320 family) that can handle about 150 passengers have a take-off and landing speed about 80 m/s. Based on this speed and the aircraft size, the respective Reynolds number is 15.5 x 10^9 , which is in the region of full turbulence.

This paper aims to conduct a preliminary analysis of the effects of various cylindrical cross-sectional shapes on vortex-induced vibration for airport runaway air wake energy generation. The simulation model is set up in ANSYS Fluent as a transient problem to solve the Navier-Stokes equations with enhanced mesh intensity to predict the flow separation and the vortex shedding phenomena using the typical frequently-used aircraft size (A320 family) as the characteristic length scale and its landing and take-off speed data.

REVIEW OF THEORY

VIV Theory

Vortex shedding is the phenomena that occur when a body submerged in a flowing fluid at the turbulence region. The fluid is viscous, so it produces flow separation due to the difference in the boundary layer along the body surface and surface roughness of the body. Most of the recent studies explained the periodic patterns of the vortex shedding that occur behind the body when the flow tends to form Kármán vortex street and investigated experimentally and numerically to enhance a better understanding on the vortex street phenomena [4]. Usually, the studies were focused on the suppression mechanism (refer to [5] for example) due to the unwanted structural vibrations.

Vortex Shedding

Reynolds number is affecting the phenomena of vortex shedding directly, which is more dependent on the free stream velocity, *U* and viscosity:

$$Re = \frac{U\,D}{v} = \frac{U\rho D}{\mu} \qquad (1)$$

where *D* is the diameter of the cross-section normal to the stream velocity direction *U*, ν and μ are the kinematic and dynamic viscosity of the fluid, respectively. Most of the recent studies are about a cylinder with circular cross-section submerged in a fluid. Three main flow regions were tested and investigated for flow over the surface under laminar flow, transition flow and turbulence flow.

Strouhal Number

The Strouhal number (*S*) is a non-dimensionless parameter that relates the vortex shedding frequency to the flowing fluid:

$$S = \frac{D\,f_s}{U} \qquad (2)$$

where f_s represent the vortex shedding frequency, *D* and *U* are cross-section diameter and free stream velocity, respectively. The Strouhal number is almost constant at about 0.2 for a wide range of Reynolds numbers between 10^3 - 10^5 [6].

Vortex-induced Vibration for Aquatic Clean Energy (VIVACE)

VIVACE was patented in 2005 at the University of Michigan to produce electricity from oscillations that occur from the water flow [7]. The system consists of a cylinder with circular cross-section submerged in flowing water that makes the system oscillates. A radial movement allows the cylinder to move once the fluid is in motion. Due to differences in lift and drag forces, the cylinders attached with magnetic sliders and coil are forced to move upward and downward. When a magnet moves over a coil, a DC-current will be produced, either could be stored or converted to AC-current. The advantage of the current patent is that it is not affecting the marine life while it generates electricity, which accounts as a renewable and environmentally friendly energy resource. It does not have any rotating equipment. Hence the possibility of fatigue or cracks is negligible. It oscillates at low stream velocity and viscosity.

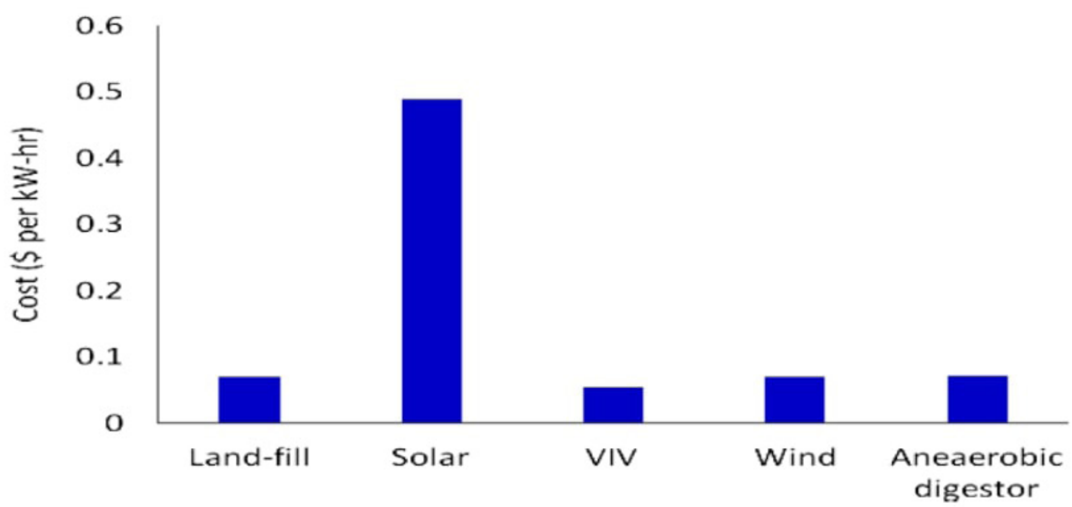

Figure 1 Cost comparison between different renewable sources of power

Compared to water turbines, VIVs are more realistic when it comes to the amount of power produced, size of the prototype, start-up costs and the produced amount of power per unit area. Figure 1 shows the cost comparison. The VIV total power costs are too close to the wind energy and other renewable energy.

The VIVACE patented to use a circular cross-section submerged on the water. However, the cross-section area can be varied to produce a greater amount of lift forces at lower speeds. This has received little attention to date due to the complexities of vortex generation.

METHODOLOGY

Models

The effect of the cross-section is investigated by considering different cases in order to find the best case that is suitable for the airport runway application at the specified condition. Five cases are simulated in ANSYS Fluent 2-D using *k-ω* turbulence model. The *k-ω* turbulence model has been discussed in Chan et al. [8]. The first case is a pure circular cross-section, and then elliptical shapes are simulated by varying the height or the length. The purpose is to identify the most efficient cross-section among the five cases by flow simulation. In addition, two extra cases of axial and radial distributions of VIV are simulated based on the best case among the five cases, to find the best orientation for potential airport applications.

The five cases are (Figure 2):

1. Circular cylinder with Diameter 2″.
2. Elliptical cylinder with major axis 2.5″ (horizontal) and minor axis 2″.
3. Elliptical cylinder with major axis 3″ (horizontal) and minor axis 2″.
4. Elliptical cylinder with major axis 2.5″ (vertical) and minor axis 2″.
5. Elliptical cylinder with major axis 3″ (vertical) and minor axis 2″.

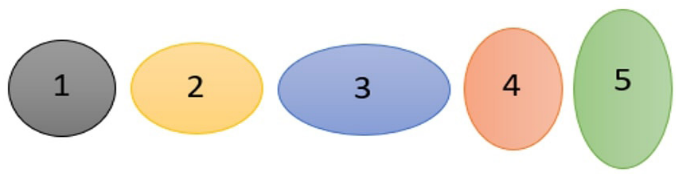

Figure 2 The five simulated cases

Meshing

Intensive mesh is utilized to create elements that will be used to solve the problem. Mesh refinement is done by minimizing the edge size of the model to 1 mm. Inflation of 1mm is set for the first boundary layer and is increased to 50 layers by a rate of 3 times [9]. The number of elements and nodes for all cases is about 24500 and 17500, respectively. Meshing independency has been justified in Chan et al. [8].

Boundary Conditions and Time Step

A transient problem is to be solved in ANSYS Fluent to predict the flow separation. The boundary condition used is the inlet velocity of the free stream. It is assumed to be 80 m/s as mentioned earlier (i.e. taking off and landing speed). The time step used was calculated to predict the minimum mesh face size, to avoid errors of floating points and to provide accurate results by dividing the minimum element size with speed used which results in a 0.001 time step [10]. The program was set to solve for 0.5 seconds.

RESULTS AND DISCUSSION

Figure 3-7 show the contours for the velocity distribution at three different timing: initial time zero second, 0.01 second and at full time 0.5 second. All cases were simulated at an inlet velocity of 80 m/s to reflect dynamic similarity for larger aeroplane speed (i.e. A320 family). Figure 3 represents Case 1 velocity contours; at the initial time, the flow interacts with the body for which asymmetrical distribution is noticeable for the lift forces. Then at time 0.01 s, the Kármán vortex street phenomena (KVSP) started to be produced. At full-time step (0.5 s), the flow will reach a steady state where it will not change even if the time increased further and the very small lift force produced can be neglected. In Case 2 (Figure 4), the pressure distribution will be interrupted since more surface will be covered, and that makes the pressure drag force reduced from the circular cross-section [11]. As noted from both Cases 2 & 3 (Figures 4-5) when the ellipse length increased further, a reduction of drag force will occur, which will make the oscillations forces weaker (Table 1). Cases 4 and 5 (Figures 6-7) represent the best two cases – the vertical elliptical cross-section provides more forces than other cases due to the height of the ellipse makes the Reynolds number variation higher than the other cases (at the same flow speed). Pressure drag is also increased due to the bluffer bodies' hence larger adverse pressure gradients. So, the additional two cases are radial, and axial distribution of four elliptical cross-sections separated linearly in a specified distance of 500 mm between each with major axis vertical of 3″ and length 2″. A spring is attached to convert the oscillation to electrical power [12]. The mass applied and spring stiffness can be found using the following equations,

$$M_{app} = \rho_{air} \times V_{cylinder} \tag{3}$$

$$k = (f_s \times 2\pi)^2 \times M_{app} \tag{4}$$

where ρ_{air} is the density of air, $V_{cylinder}$ is the volume of the cylinder, k is the spring stiffness constant, f_s is the shedding frequency, and M_{app} is the total mass applied in the system.

The natural frequency of oscillation (f_N) required to find the total power produced from one-unit length:

$$f_N = \frac{1}{2\pi}\sqrt{\frac{k}{m_{app}}} \tag{5}$$

$$P(t) = v(t)\, F_L \sin(2\pi f_N t) \tag{6}$$

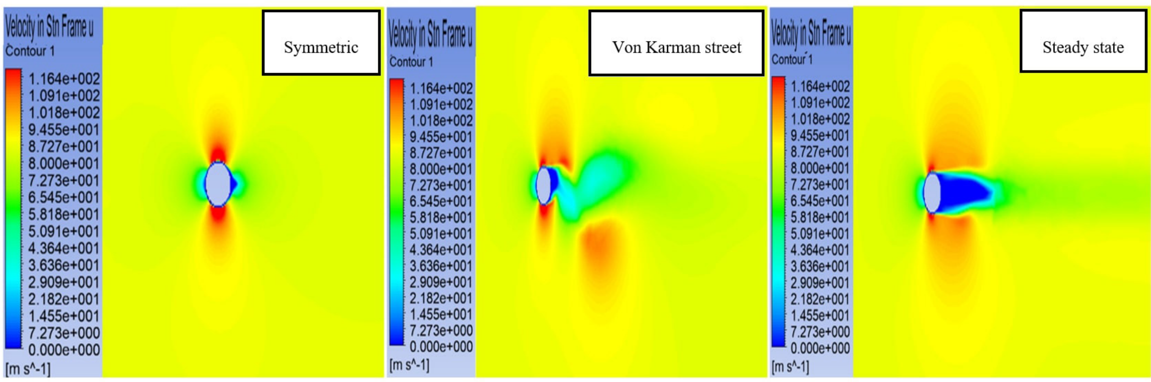

(a) (b) (c)

Figure 3 Velocity contours of Case 1 at, a) zero time, b) 0.01 second, c) at full time

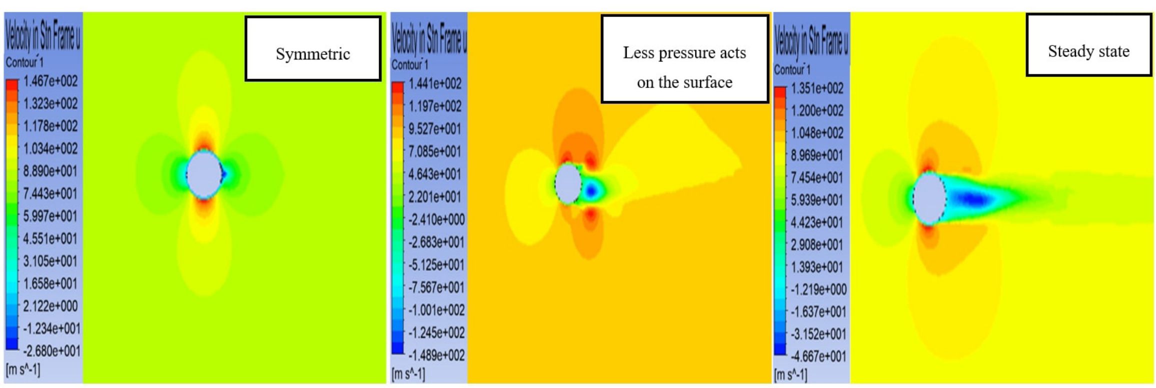

(a) (b) (c)

Figure 4 Velocity contours of Case 2 at, a) zero time, b) 0.01 second, c) at full time

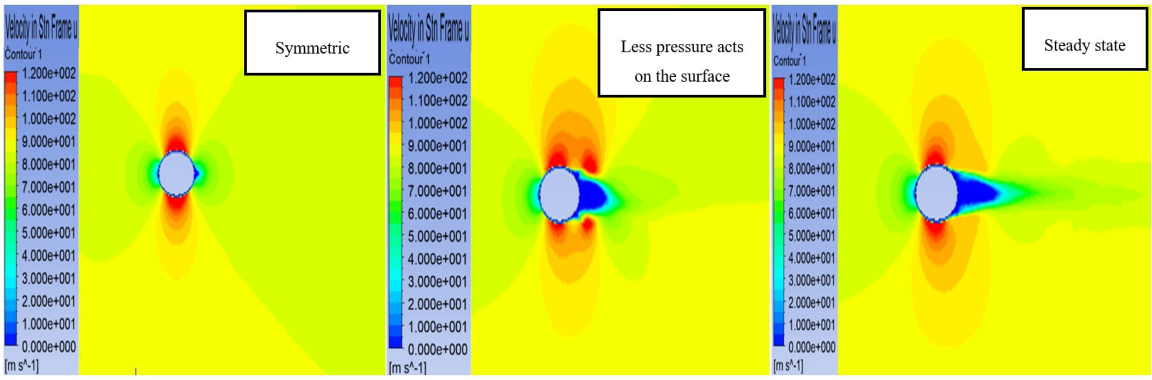

(a) (b) (c)

Figure 5 Velocity contours of Case 3 at, a) zero time, b) 0.01 second, c) at full time

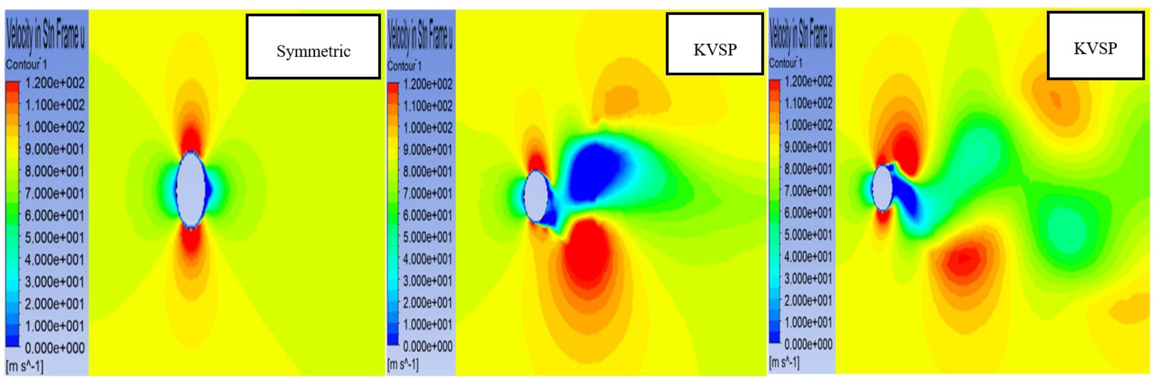

(a) (b) (c)

Figure 6 Velocity contours of Case 4 at, a) zero time, b) 0.01 second, c) at full time

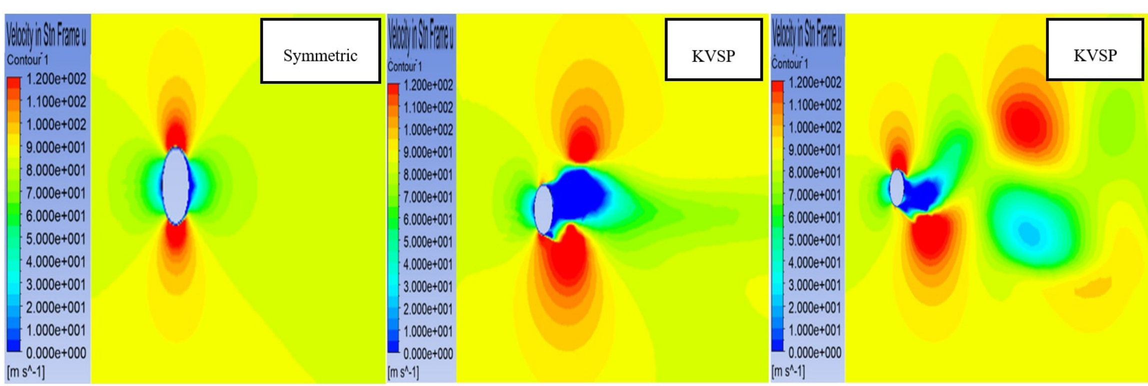

(a) (b) (c)

Figure 7 Velocity contours of Case 5 at, a) zero time, b) 0.01 second, c) at full time

Table 1 ANSYS drag and lift forces

Comparison	Drag Force (N)	Lift Force (N)	Applicable\Not applicable
Case 1	79.6	6.4	Not Applicable (small lift force)
Case 2	49.3	7.3	Not Applicable (small lift force)
Case 3	35.2	4.3	Not Applicable (small lift force)
Case 4	466.4	388.6	Applicable (High lift force)
Case 5	574.2	707.8	Applicable (Highest lift force)

Additional Cases 6 and 7

The most efficient vortex-induced vibration for larger energy generation among the provided cases is for Case 6 (3"& 2"). Its drag and lift forces are 1.3947 kN and 2.9535 kN, respectively. For Case 7, the drag is 1.6778 kN and lift of 1.8671 kN. Figures 8 and 9 illustrate the velocity contours for Case 6 and Case 7, respectively.

The reason that Case 6 has better oscillation performance when compared to Case 7 is that the turbulent inlet flow reaches all bodies at the maximum speed and uniformly distributed. The high stream velocity makes air at low viscosity to generate forces, which implies that VIV is a useful energy source to be applied at the airport busy runaways. However, the axial distribution reaches the first body at maximum speed, but once it passes, the flow will be interrupted; hence it will not produce high lift forces comparatively.

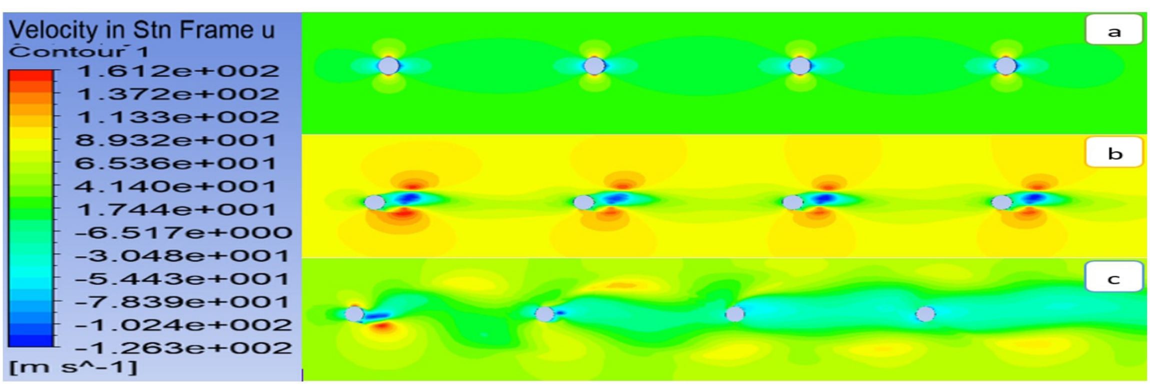

Figure 8 Velocity contour of Case 6 at, a) zero time, b) 0.01 second, c) at full time

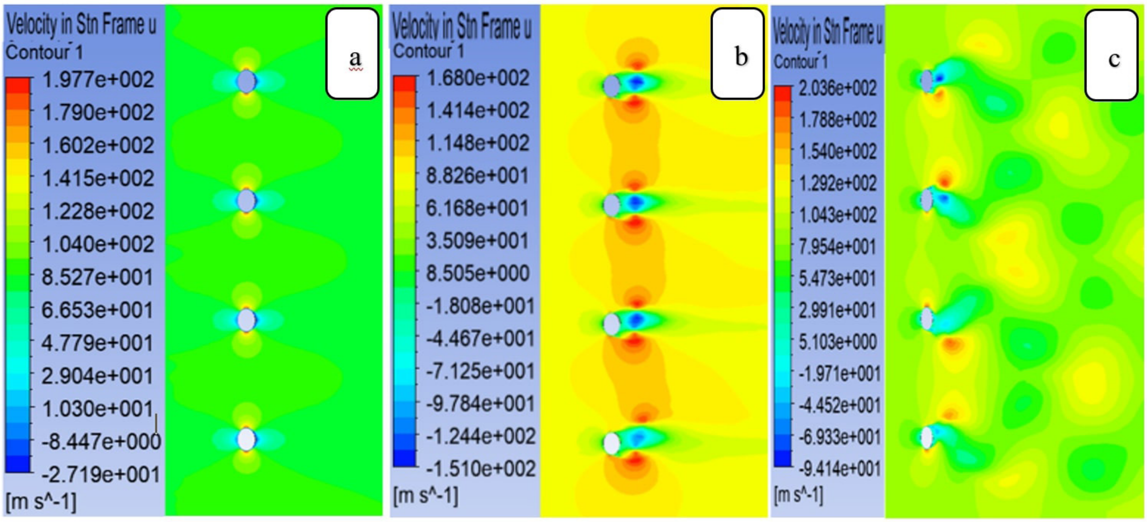

Figure 9 Velocity contour of Case 7 at, a) zero time, b) 0.01 second, c) at full time

Table 2 shows the lift force and drag force obtained from ANSYS Fluent after 30 iterations on each time step.

Table 2 Results in additional cases

Comparison	Case 6	Case 7
Drag Force (N)	1394.7	1677.8
Lift Force (N)	2953.5	1867.1

Final Design

The final render of vortex-induced vibration for airport runaway air wake energy generation was modelled in ANSYS Workbench. The converter from mechanical oscillations to electric energy was attached, which had a specified distance taking into consideration the shedding frequency. Figure 10 shows the isometric view and side view of the final render. The length of each elliptical cylinder is 1 meter, and the distance between each elliptical cylinder is 0.5 m. All the elliptical cylinders are connected to a cylinder at

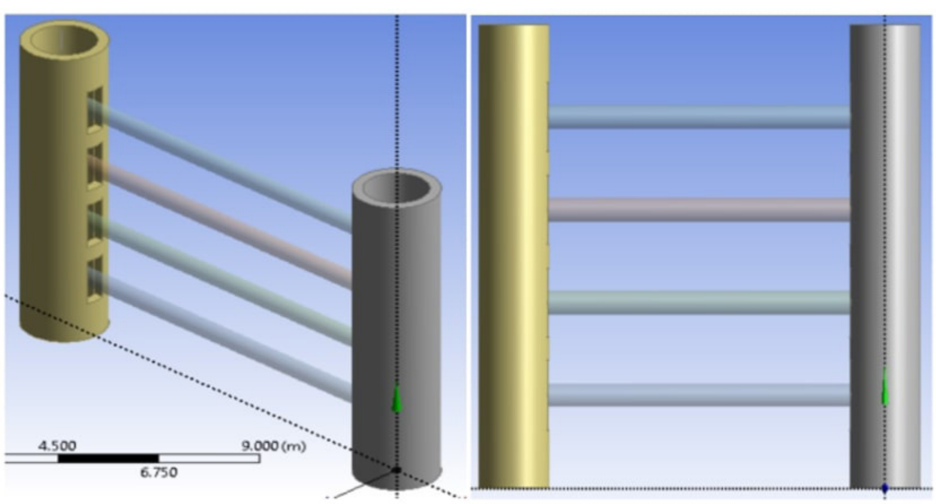

Figure 10 Final render of VIV

both ends, which consists of springs that convert the mechanical oscillation to electrical power. The results are summarized in Table 3. To validate the result outcomes the image of velocity fields obtained and analysed using a technique called wavelet-based optical velocimetry [13]-[14].

Table 3 Analytical calculation based on a single-cylinder system

Case	1	2	3	4	5
Reynolds number (x 10^{5})	2.9176	2.9176	2.9176	3.647	4.3764
Shedding frequency, Hz	334.7	334.7	334.7	267.8	223.1
Volume (x 10^3), m^3	2.027	2.534	3.040	2.534	3.040
Mass applied, kg	0.00248	0.00310	0.00372	0.00310	0.00372
Spring stiffness, kN/m	10.96	13.7	16.44	8.77	7.29
Natural frequency, Hz	334.5	334.5	334.5	267.6	222.8
Drag coefficient	0.02	0.02	0.018	0.05	0.035
Lift coefficient	0.0025	0.008	0.005	0.0225	0.07
Total power, W	30	135.4	95.3	309.7	707.1

CONCLUSION

VIV can be used as a useful renewable energy source. It has the ability to provide energy even for low viscosity fluid such as air. The preliminary results show that airport runway operations (landing and taking off or aeroplanes) provide sufficient VIV forces to be converted to useful energy. The energy generated is more consistent, and it just depends on the runaway operations, which is expected to grow with time for every airport. The elliptical shapes with larger heights generate more force and power than those that have a longer length, and the observed results from simulations showed that the ellipse with 3" height and 2" length is the best case among other tested cases. The total power produced from single-cylinder with a small cross-section per unit one meter can provide 707.1 W within 0.5 seconds. The system can be optimized for larger aeroplanes and operation frequencies as well as could be expanded for larger energy output. In future, specific airports can be studied by investigating the frequency between two aeroplanes for take-off or landing operations and the volume of air-traffics. This can then be applied as a variable inlet in ANSYS Fluent to develop better results. Dynamic meshing can also be applied to verify the effects of having multiple cross-sections.

REFERENCES

[1] Y.K. Tiong, M.A. Zahari, S.F. Wong & S.S. Dol, "The feasibility of wind and solar energy application for oil and gas offshore platform", In *IOP Conference Series: Materials Science and Engineering*, 78, 1, p. 012042, 2015.

[2] M.A. Zahari & S.S. Dol, "Application of vortex induced vibration energy generation technologies to the offshore oil and gas platform: The preliminary study", *International Journal of World Academy of Science, Engineering and Technology*, 8, 7, pp. 1331-34, 2014.

[3] H. Morris, "An airport just broke the record for most flights handled in a single day", 27 November 2017. [Online]. Available: https://www.telegraph.co.uk/travel/destinations/asia/india/articles/busiest-airport-in-world-aircraft-movements/.

[4] S.S. Dol & M.A.M. Nor, "Flow visualization of the vortex shedding of a stationary circular cylinder by an improved smoke-wire technique," *WSEAS Transactions on Fluid Mechanics*, 1, 6, p. 745, 2006.

[5] S.S. Dol. "Weakened vortex shedding from a rotating cylinder", *International Journal of Mechanical and Mechatronics Engineering*, 7, 10, pp. 2013-2020, 2013.

[6] A.K. Soti, M.C. Thompson & J. Sheridan, "Electrical power generation from vortex induced vibration of a circular cylinder", in *20th Australian Fluid Mechanics Conference*, Perth, Australia, 2016.

[7] M. Barnitsas & K. Raghavan, "Fluid Motion Energy Convertor". Patent U.S. Patent Serial No. 11\272, p. 504, 2005.

[8] H.B. Chan, T.H. Yong, P. Kumar, S.K. Wee & S.S. Dol. "The numerical investigation on the effects of aspect ratio and cross-sectional shape on the wake structure behind a cantilever", *Journal of Engineering and Applied Sciences,*11, 16, pp. 9922-932, 2006.

[9] A.A. Azeez, M. Gadala, N. Al Khudhiri & S.S. Dol, "Aerodynamics Optimization of RC Plane Winglet", in *2019 8th International Conference on Modeling Simulation and Applied Optimization (ICMSAO),* IEEE, pp. 1-5, 2019.

[10] S.S. Dol, H.B. Chan, S.K. Wee & K. Perumal, "The effects of flexible vortex generator on the wake structures for improving turbulence", In *IOP Conference Series: Materials Science and Engineering*, 715, 1, p. 012070, 2020.

[11] M. Zahari & S.S. Dol, "Alternative energy using vortex-induced vibration from furbulent flows: Theoretical and analytical analysis", in *5th Brunei International Conference on Engineering and Technology (BICET 2014),* IEEE, 2014.

[12] M. Zahari, H. Chan, T. Yong & S.S. Dol , "The Effects of Spring Stiffness on Vortex-Induced Vibration for Enerrgy Generation", in *IOP Conference Series: Materials Science and Engineering*, 78, p. 012041, 2015.

[13] A.B. Osman & M. Ovinis. "Evaluation of k-epsilon model for turbulent buoyant jet", *Platform: A Journal of Engineering* 3, 2, pp. 55-64, 2019.

[14] A.B. Osman, M. Ovinis, F.M. Hashim & I. Faye. "Wavelet-based optical velocimetry for oil spill flow rate estimation", *Measurement*, 138, pp. 485-496, 2019.